International Journal of Electronics
Publication details, including instructions for authors and subscription information:
http://www.tandfonline.com/loi/tetn20

CMOS prototype for retinal prosthesis applications with analog processing

G. Castillo-Cabrera[a], J. García-Lamont[b], M.A. Reyes-Barranca[c], Y. Matsumoto-Kuwabara[c], J.A. Moreno-Cadenas[c] & L.M. Flores-Nava[c]
[a] ESCOM-IPN, Mexico City, Mexico
[b] UAEH, Pachuca, Mexico
[c] CINVESTAV-IPN, Zacatenco, Mexico

Accepted author version posted online: 31 Jan 2014.Published online: 24 Feb 2014.

To cite this article: G. Castillo-Cabrera, J. García-Lamont, M.A. Reyes-Barranca, Y. Matsumoto-Kuwabara, J.A. Moreno-Cadenas & L.M. Flores-Nava (2014) CMOS prototype for retinal prosthesis applications with analog processing, International Journal of Electronics, 101:12, 1621-1646, DOI: 10.1080/00207217.2014.888776

To link to this article: http://dx.doi.org/10.1080/00207217.2014.888776

International Journal of Electronics, 2014
Vol. 101, No. 12, 1621–1646, http://dx.doi.org/10.1080/00207217.2014.888776

Taylor & Francis
Taylor & Francis Group

CMOS prototype for retinal prosthesis applications with analog processing

G. Castillo-Cabrera[a]*, J. García-Lamont[b], M.A. Reyes-Barranca[c], Y. Matsumoto-Kuwabara[c], J.A. Moreno-Cadenas[c] and L.M. Flores-Nava[c]

[a]*ESCOM-IPN, Mexico City, Mexico;* [b]*UAEH, Pachuca, Mexico;* [c]*CINVESTAV-IPN, Zacatenco, Mexico*

(*Received 16 October 2012; accepted 10 November 2013*)

A core architecture for analog processing, which emulates a retina's receptive field, is presented in this work. A model was partially implemented and built on CMOS standard technology through MOSIS. It considers that the receptive field is the basic unit for image processing in the visual system. That is why the design is concerned on a partial solution of receptive field properties in order to be adapted in the future as an aid to people with retinal diseases. A receptive field is represented by an array of 3×3 pixels. Each pixel carries out a process based on four main operations. This means that image processing is developed at pixel level. Operations involved are: (1) photo-transduction by photocurrent integration, (2) signal averaging from eight neighbouring pixels executed by a neu-NMOS (ν-NMOS) neuron, (3) signal average gradient between central pixel and the average value from the eight neighbouring pixels (this gradient is performed by a comparator) and finally (4) a pulse generator. Each one of these operations gives place to circuital blocks which were built on 0.5 μm CMOS technology.

Keywords: receptive field analog pixel processing; ν-NMOS neuron

1. Introduction

In the retina, the basic processing unit is called *receptive field* (RF). They are found throughout all stages of the optic pathway. On each stage, several topologies for RF are found (circular, elliptical or elongated) (Hubel & Wiesel, 1959, 1962). However, circular RFs are commonly found in the retina. The classical model and the ideal model for the retina with a circular topology for RFs are shown in Figure 1. The ideal model for a RF is described by two concentric regions, one called 'centre' and the other 'surround'. For example, each horizontal cell has a RF that consists of photoreceptors, cones or rods or both (Zhang & Wu, 2009). In the case of ganglion cells, each one of these cells has a RF and consists of bipolar and amacrine cells. From the interaction between those regions, several interesting properties arise which determine the visual processing in the retina. The most known are summarised in Table 1 (Chen, Weng, Deng, Xu, & He, 2009; Cleland, Dubin, & Levik, 1971; Ichinose & Lukasiewicz, 2005; Kilavik, Silveira, & Kremers, 2003). Particularly, this work deals with the design of the so-called 'ON' centre with sustained and transient response.

The biological protocol for optical signal processing in the retina is explained with the help of Figures 2 and 3, where, two opposite conditions are shown, i.e. one when only the

*Corresponding author. Email: gcastilloc@ipn.mx

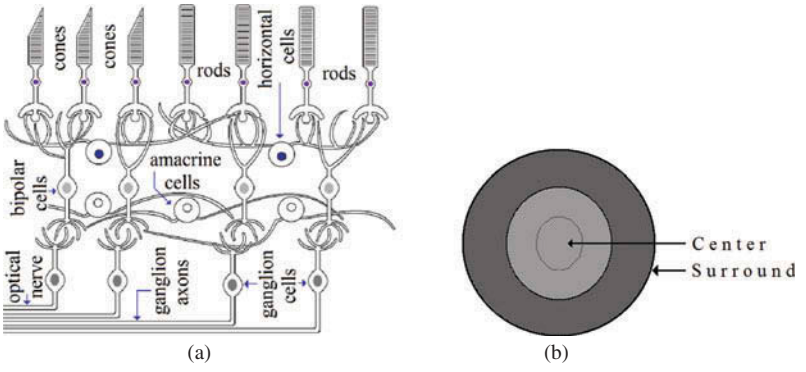

Figure 1. (a) Retinal's classical topology; (b) Ideal circular topology for a receptive field.

Table 1. Classification of receptive fields.

Receptive field	Type of response
'ON' centre with	Sustained response
	Transient response
'OFF' centre with	Sustained response
	Transient response

centre is illuminated and other when only the surround is illuminated. However, in practice, whether the centre or the surrounding of a RF is more illuminated can be determined through gradient computations, in a wide continuous range of illumination. Figure 2(a) – **Sustained response** (**A STATES**): When the light spot is turned on and falls over the region called centre, the neuron is fired. It defines the A STATE 'ON' (*current state*). The rate of firing is constant for a certain time while the light spot is turned on. After that, the neuron is turned off when the light spot is turned off and a low rate of residual only firing remains. It defines the A STATE 'OFF' (*following state*). (**B STATES**): When the light spot is turned on and falls over the surrounding, the neuron remains off, however with a weak response that is attributed to the scene's background. It defines the B STATE 'OFF' (*current state*). After that, if the light spot is turned off, the

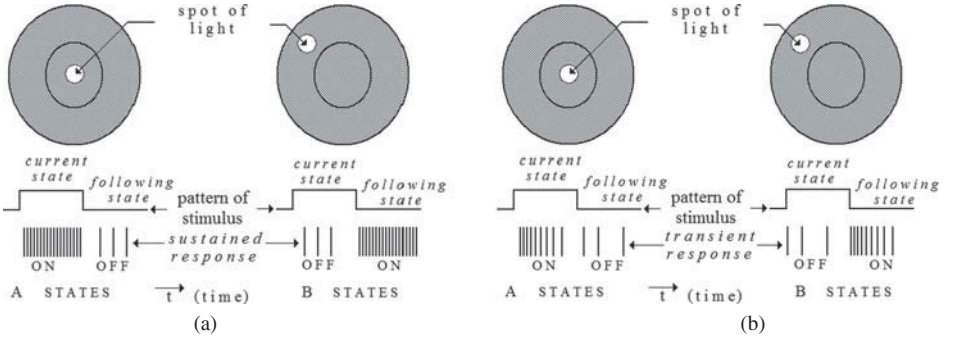

Figure 2. Receptive field's response type ON: (a) sustained; (b) transient.

neuron is turned on. In this case, the pulse rate is constant during a certain time. That time is related to the latency of a neuron. It defines the B STATE 'ON' (*following state*).

Figure 2(b): **Transient response** (**A STATES**): When a light spot is turned on and falls over the region called centre, the neuron is fired with a kind of transient response. It defines the A STATE 'ON' (*current state*), as shown in the figure. The initial response is high and proportional to the magnitude of illumination and it decreases with time even though the light spot is on. After that, the neuron is turned off also when the light spot is turned off, and a low rate of firing only remains. It defines the A STATE 'OFF' (*following state*). (**B STATES**): When the light spot is turned on and falls over the surrounding, the neuron remains off, however with a low rate of residual firing that is attributed to the scene's background. It defines the B STATE 'OFF' (*current state*). After that, when the light spot is turned off and falls over the surrounding, the neuron is fired with a kind of transient response during a certain time. That time is related to the latency of a neuron. It defines the B STATE 'ON' (*following state*).

So far, we have described the qualitative neural protocol in the case of a 'receptive field type ON centre' which is represented in Figure 2(a) and (b) and an explanation was given for a sustained and a transient response. Now, we will give a description for the case of 'Receptive Field type OFF centres' (Figure 3) with sustained (a) and transient (b) response.

Figure 3(a) – **Sustained response** (**A STATES**): When the light spot is turned on and falls over the region called centre, the neuron remains off, however with a weak response that is attributed to the scene's background. It defines the A STATE 'OFF' (*current state*) as is shown in the figure. After that, the neuron is fired on when the light spot is turned off. The response is constant over a given time interval which is related to the latency of a neuron. It defines the A STATE 'ON' (*following state*). (**B STATE**): When the light spot is turned on and falls over the region called surround, the neuron is turned on. The response is constant over time while the spot is on, as is shown at the right of Figure 3(a). Then, the neuron is turned off also when the light spot is turned off, however with a weak response. It defines the B STATE 'OFF' (*following state)*.

Figure 3(b) – **Transient response** (**A STATES**): When the light spot is turned on and falls over the region called centre, the neuron remains off, however with a weak response what is attributed to the scene's background. It defines the A STATE 'OFF' (*current state*) as is shown at the left of Figure 3(b). Then, the light spot is turned off and the neuron is fired, with a kind of transient response during a time which is related to latency of the

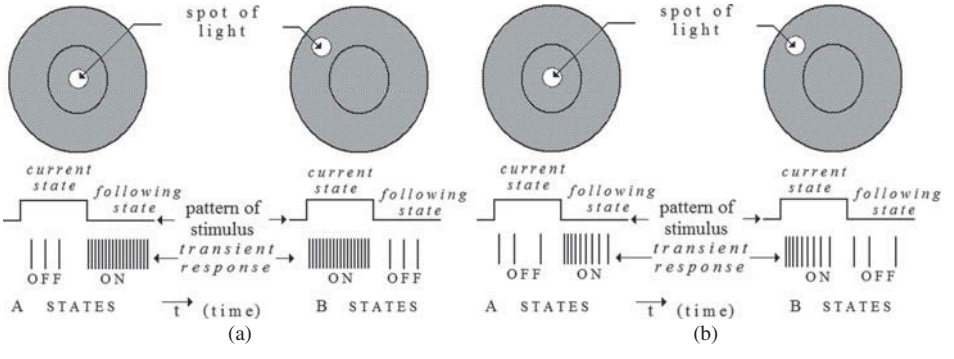

Figure 3. Receptive field's response type OFF: (a) sustained; (b) transient.

neuron. It defines the A STATE 'ON' (*following state*). (**B STATES**): When light spot is turned on and falls over the region called surround, the neuron is fired with a kind of transient response. It defines the B STATE 'ON' (*current state*). Then, the light spot is turned off, and the neuron is turned off also; however a weak response remains as is shown at the right of Figure 3(b).

The models in Figures 2 and 3 are supported with reported measurements made by several researchers throughout many years, from 1938 by Hartline (Hartline, 1938), until recent years from 2003 to 2009 (Chen et al., 2009; Ichinose & Lukasiewicz, 2005; Kilavik et al., 2003).

2. Model

In this section, a mathematical model for ON and OFF centres with sustained and transient responses is presented. It is the simplest, quickest and easiest model to be implemented on hardware at a transistor level. Thereby, a pixel was designed having four modules as shown in Figure 4. For analysis purpose, a RF is represented by one 3×3 pixel array (Figure 5); thus, its operation starts with the identification of magnitude and direction of the gradient between the centre and the surround.

The first block in Figure 4 represents a *photo-transducer*, which translates optic signal in electric; the *Comparator* block represents the analog comparator; *The v-NMOS neuron* is an analog adder, which adds weighted signals from neighbours with the signal from photo-transducer in the local pixel; finally, the *Oscillator* is the spikes generator. Each one of these processing blocks is described in Section 4. Actually, the blocks were generated from the mathematical model as will be explained in the cited Section 4. Let V_k be the kth voltage response of the kth photoreceptor in the kth pixel in the array is shown in Figure 5. This is the minimum possible array for signal processing of a RF. Pixel 5 will be called 'central pixel' and represents the centre of the RF. The remaining pixels represent the surrounding of the RF and will be called 'pixels of surround'. Besides, V_Ω is the average voltage of the surrounding eight pixels and it is obtained with the following equation:

$$V_\Omega = \left(\sum_{k=1}^{8} V_k\right) \Big/ 8 \tag{1}$$

Next, ΔV_0 is the voltage gradient and is simply:

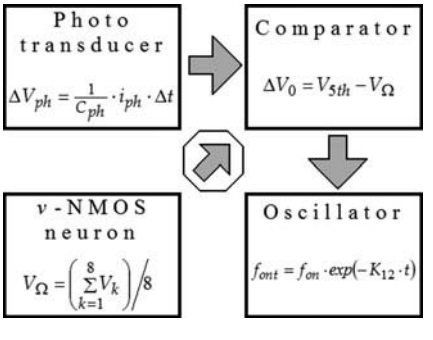

Figure 4. Block diagram for each pixel.

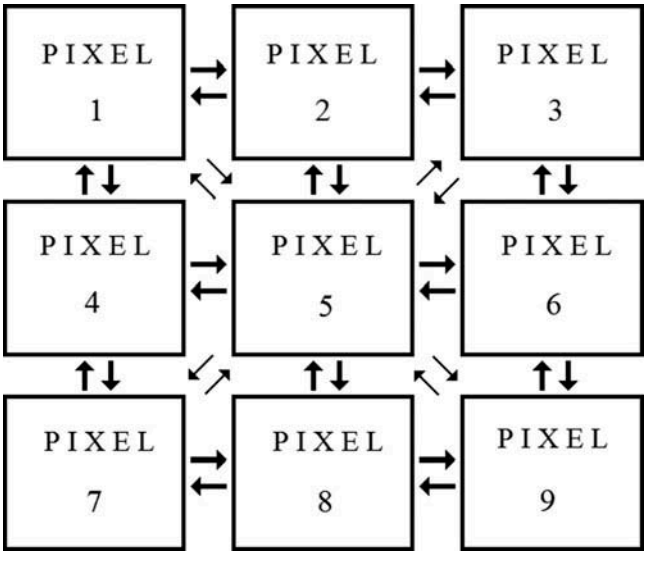

Figure 5. Receptive field represented by an array of 3×3 pixels.

$$\Delta V_0 = V_{5th} - V_{\Omega} \tag{2}$$

Each V_{th} voltage is the initial value present just after a short sample is taken with an electronic shutter, then, ΔV_0 is the initial voltage gradient just after this sampling. A new parameter, δ, named threshold is defined and if $\delta > 0$ the neuron is fired depending on the value of ΔV_0. Now are presented several possible associated cases to the kind of RFs; these cases are shown in Table 2.

In a first stage of this research and for simplicity, this work is concerned on implementing only cases 1-I, 1-II, 1-III, 2-I, 2-II and 2-III, belonging to the *current state* condition, since each case could become a more complex one if they must be implemented in a silicon integrated circuit. Implementation of *current states* and *following states* simultaneously could imply an analog sequential analysis like in digital circuit analysis; however the model in Table 2 is analog.

3. Simulation in Matlab

A first simulation was done under Matlab Simulink, with embedded Matlab functions and user-defined functions. This was carried out based on the model shown in Figure 5 and Table 2. The function is illustrated in Figure 6. Simulations were done using eight-bit digital inputs. Inputs and the average are controlled with the blocks named 'gain' and 'sum of elements', respectively. The pulsed response of these blocks is programmed into the block named 'onfm' having an output dependent on input 'x'. The results obtained were expected, according to the mathematical model established before. Figure 7 shows a typical result for a transient response in agreement to what was previously specified for an ON centre Although it is a digital simulation, it has the main properties of RFs which belong to the model and have been carefully included in block 'onfm'.

At this point an intrinsic property of the model can be identified, this is that sustained responses can be considered as particular transient cases when measurement is done

Table 2. Model for 'ON' and 'OFF' receptive field centre.

Cases	Sub-cases	Condition	State	Response
1. ON centres with sustained response	1-I A-STATES	$\Delta V_0 > \delta$	Current state	$f_{1-I} = K_{1-I} \cdot \Delta V_0$
			Following state	Weak function of contrast with background of scene
	1-IIB-STATES	$\Delta V_0 < -\delta$	Current state	Weak function of contrast with background of scene
			Following state	$f_{1-II} = K_{1-II} \cdot \Delta V_0$
	1-III C-STATES	$-\delta < \Delta V_0 < \delta$	Current state	$f_{1-III} = K_{1-III} \cdot \Delta V_0$
			Following state	Weak function of contrast with background of scene
2. ON centres with transient response	2-I A-STATES	$\Delta V_0 > \delta$	Current state	$f_{2-I} = f_{1-I} \cdot \exp(K_{2A} \cdot t)$
			Following state	Weak function of contrast with background of scene
	2-II B-STATES	$\Delta V_0 < -\delta$	Current state	Weak function of contrast with background of scene
			Following state	$f_{2-II} = f_{1-II} \cdot \exp(K_{2B} \cdot t)$
	2-III C-STATES	$-\delta < \Delta V_0 < \delta$	Current state	$f_{2-III} = K_{2-III} \cdot \Delta V_0$
			Following state	Weak function of contrast with background of scene
3. OFF centres with sustained response	3-I A-STATES	$\Delta V_0 > \delta$	Current state	Weak function of contrast with background of scene
			Following state	$f_{3-I} = K_{3-I} \cdot \Delta V_0$
	3-II B-STATES	$\Delta V_0 < -\delta$	Current state	$f_{3-II} = K_{3-II} \cdot \Delta V_0$
			Following state	Weak function of contrast with background of scene
	3-III C-STATES	$-\delta < \Delta V_0 < \delta$	Current state	Weak function of contrast with background of scene
			Following state	$f_{3-III} = K_{3-III} \cdot \Delta V_0$
4. OFF centres with transient response	4-I A-STATES	$\Delta V_0 > \delta$	Current state	Weak function of contrast with background of scene
			Following state	$f_{4-I} = f_{3-I} \cdot \exp(K_{4A} \cdot t)$
	4-II B-STATES	$\Delta V_0 < -\delta$	Current state	$f_{4-II} = f_{3-I} \cdot \exp(K_{4B} \cdot t)$
			Following state	Weak function of contrast with background of scene
	4-III C-STATES	$-\delta < \Delta V_0 < \delta$	Current state	Weak function of contrast with background of scene
			Following state	$f_{4-III} = K_{4-III} \cdot \Delta V_0$

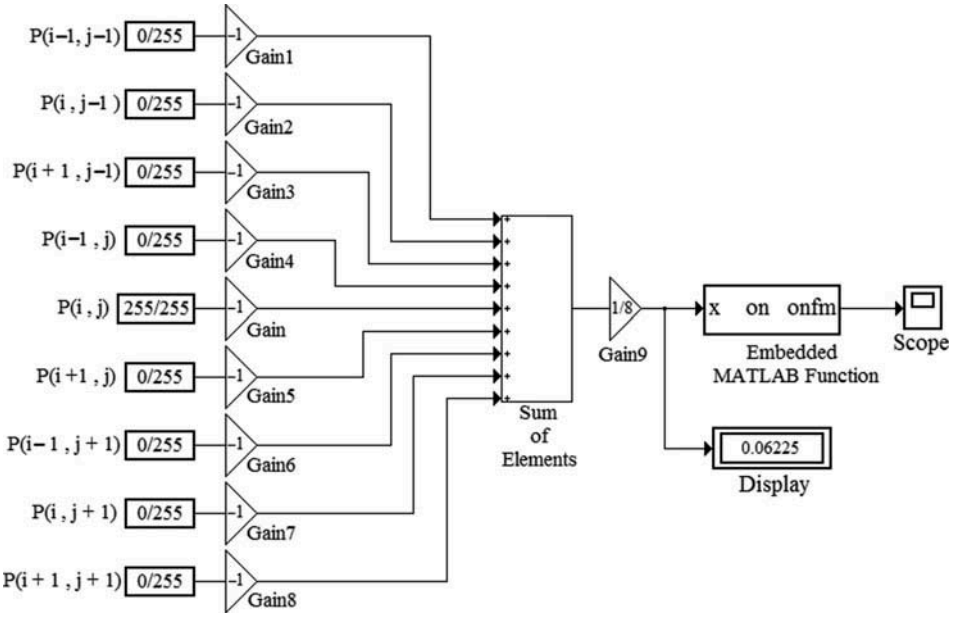

Figure 6. Embedded Matlab functions under Matlab Simulink emulating a receptive field.

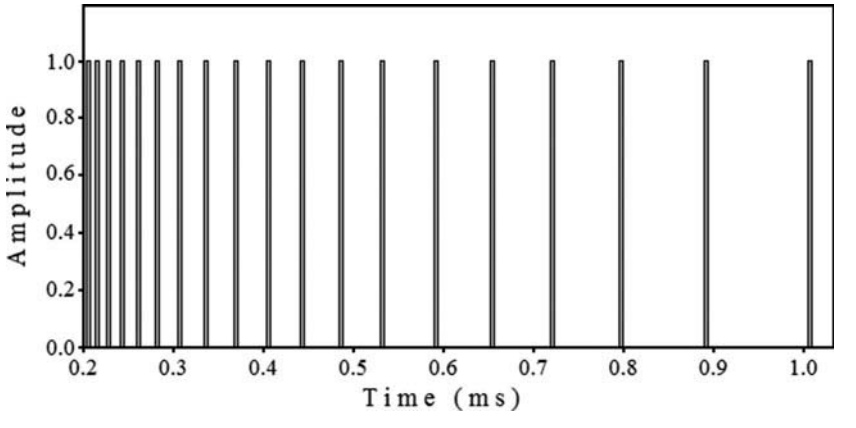

Figure 7. Simulation under Matlab Simulink. $\Delta V_0 > \delta$, ON centre.

within a time window Δt or simply t, which is shorter than latency, and such measurement is carried out after the involved neuron has been fired. Moreover, these implications can lead to the following interpretation: would imply that moving images can be analysed when the involved time is equal to or larger than latency, and each measurement is considered as a frame. However, such interpretation could be proved in future works. Following, some results are shown related to ON and OFF centres. Figure 8 is a photo from windows vista, used for the analysis. Figure 9 shows a filtered image after applying the algorithm to an ON centre with transient response, covering cases 2-I, 2-II and 2-III in Table 2, only for the conditions called *current states* and their respective equations stated

Figure 8. Original image filtered to a grey scale.

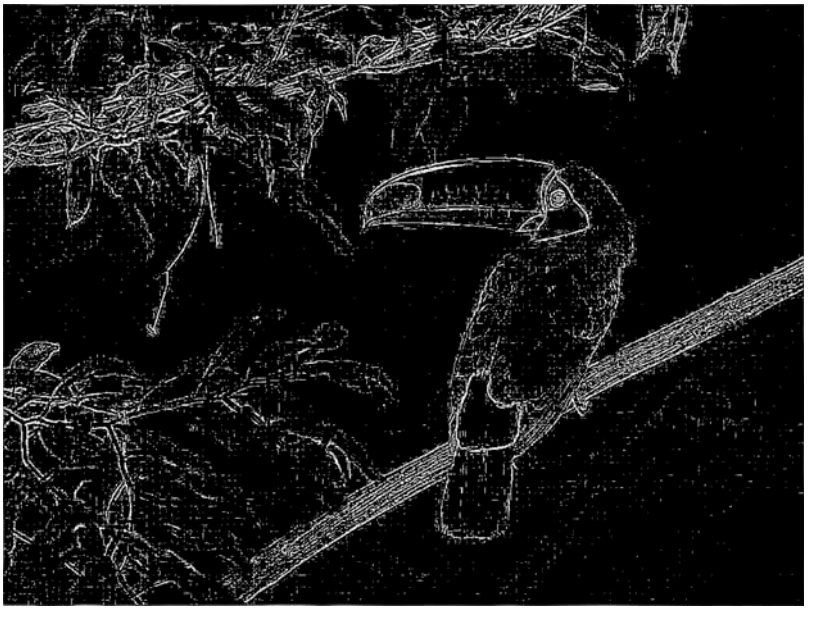

Figure 9. Simulation for cases 2-I, 2-II and 2-III in Table 2, only for the conditions called current states.

in Table 2, evaluated at $t = 0$. Figure 10 shows the same cases, but for $t > 0$ (for instance, 100 ms). Figure 11 shows a filtered image after applying the algorithm to an OFF centre with transient response, covering cases 4-I, 4-II and 4-III in Table 2, only for the

Figure 10. Simulation for cases 2-I, 2-II and 2-III in Table 2, for $t > 0$.

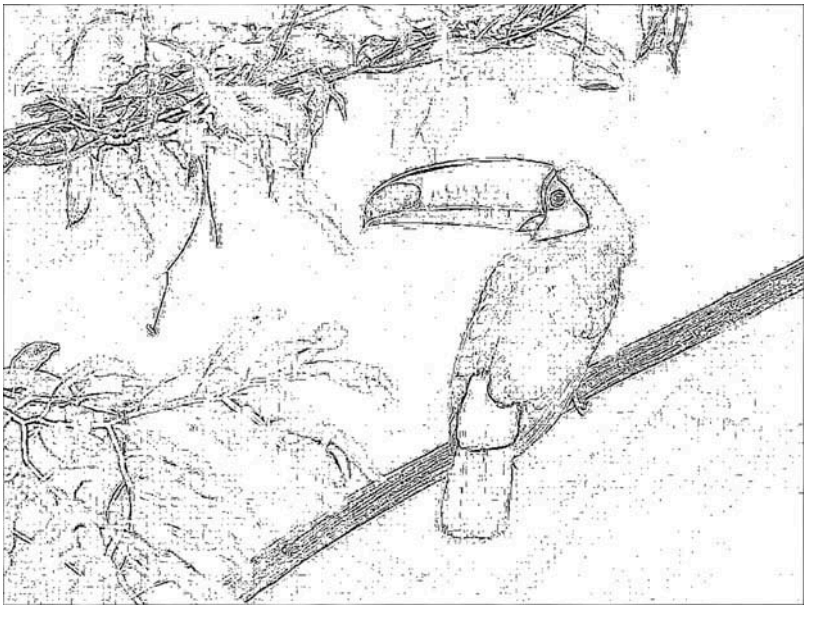

Figure 11. Simulation of cases 4-I, 4-II and 4-III in Table 2, only for the conditions called current states.

conditions called *current states* and their respective equations stated in Table 2, evaluated at $t = 0$. Figure 12 shows the same cases, but for $t > 0$ (for instance, 100 ms).

The results from previous simulations are very interesting and promising, since it rises as a biological model based on a simple and friendly algorithm for image filtering.

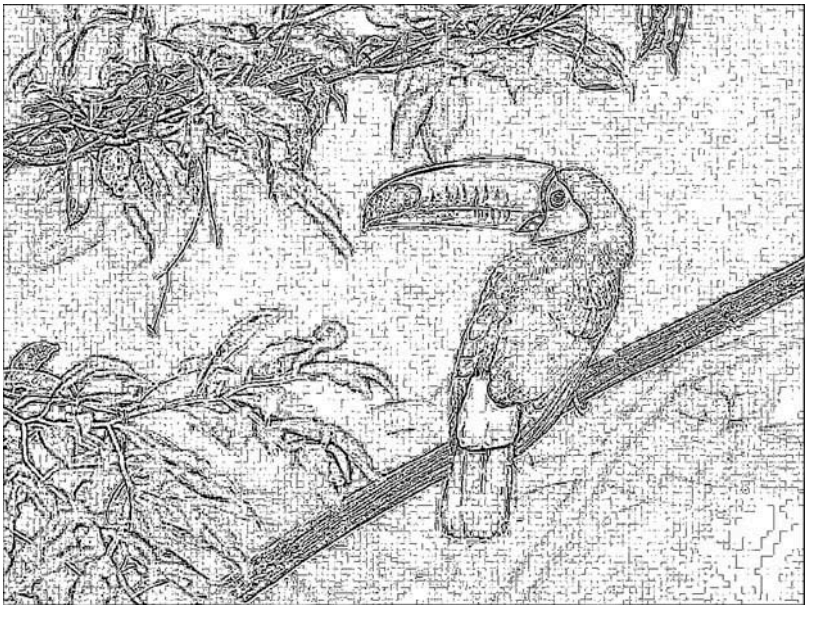

Figure 12. Simulation of cases 4-I, 4-II and 4-III in Table 2, for $t > 0$.

Moreover, as time increases, much more information is delivered in the simulation, as can be confirmed from Figures 9 to 12.

Figure 11 shows the simulation of a filtered image after applying the algorithm to an OFF centre with transient response, covering cases 4-I, 4-II and 4-III, only for conditions called *current states* and their respective equations in Table 2, evaluated at $t = 0$. Figure 12 shows the same cases, but for $t > 0$ (for instance, 100 ms).

When the image processing time (P-T) is larger, the image becomes blurry or even lost, irrespective of whether the analysis is made using ON or OFF centres. The useful parameters for performance evaluation are ΔV_0 and t. The influence is similar if either ΔV_0 or t is changed since the image can be done blurry or neat no matter either of which is changed. However, both have a different analysis approach since when only ΔV_0 is the variable, there is a stationary analysis, but on the other hand, when t is the variable, there is a transient analysis; so it is important to define in which domain the analysis has to be made.

4. Design

The model that is the core of the design is given in Section 2. That is the prototype of the RF. The architecture is supported by a mathematical model that is also given in Section 2. This is an analog processing inspired on a biological neuron with the following concerns: (1) it must avoid digital processing which implies an analog to digital conversion, (2) it must avoid external component for processing outside the chip and (3) it should perform as close as possible to the biological processing. Although, the main goal of this work is focused on the RF, most of the mathematical operations are carried out at a pixel level. So, this stage comprises the description of the designed modules. Each pixel has four operator modules that have been derived from the equations in Table 3.

Table 3. Mathematical model for sub-circuits inside each pixel.

Mathematical model	Associated sub-circuit
$V_\Omega = \frac{1}{8}\sum_{k=1}^{8} V_k$	Operation carried out by a ν-NMOS neuron, shown in Figures 3 and 4
$\Delta V_0 = V_{5\text{th}} - V_\Omega$	Achieved by a dynamic comparator, shown in Figure 3
$f_{\text{ont}} = f_{\text{on}} \cdot \exp(-K_{12} \cdot t)$	Low-frequency voltage-controlled oscillator for pulsed generator, given in Figure 3
$\Delta V_{\text{ph}} = \frac{1}{C_{\text{ph}}} \cdot i_{\text{ph}} \times \Delta t$	Integration carried out by a photo-transducer module, shown in Figure 3

Parameters in Table 3 are as follows. V_k is the kth voltage value from the neighbour pixels in the surrounding of RF, including the central pixel (PIXEL 5 in Figure 5). On each term in the mathematical model (Section 2), the illumination intensity is translated to voltage ΔV_{ph} by the transducer, then it is renamed as V_k. V_Ω is the arithmetic average value in neighbour pixels. $V_{5\text{th}}$ is the voltage value at the central pixel. The f_{on} term is the same as f_{1-I} in Table 2. The photocurrent is denoted by i_{ph} and the parasitic capacitance by C_{ph} which integrates photocurrent as photovoltage ΔV_{ph}, by assuming that i_{ph} is constant during time.

To understand the way in which the proposed architecture operates, each of its main modules (Table 3) will be explained in the following sections based on the architecture shown in Figure 13. It shows the general architecture in a block diagram for each pixel, according to a top-down methodology. The coupler modules have the role of matching their respective voltage swing windows, in both cases either between the ν-NMOS and the comparator modules or between the comparator and the oscillator modules (Figure 13). So, a pixel with a general architecture as that displayed in Figure 13 emulates a ganglion cell neuron in the retina.

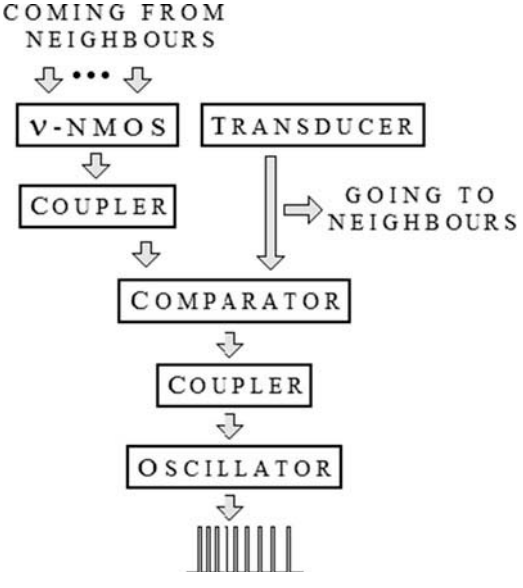

Figure 13. Architecture of each pixel.

4.1. *CMOS architecture for the ν-NMOS neuron*

The operation of the ν-NMOS neuron is based on the operation principles of a floating gate MOS (FGMOS) transistor (Shibata & Ohmi, 1992). However, the structure shown in the Figure 14 is not exactly a FGMOS transistor, but a *quasi*-FGMOS transistor (Ramírez-Angulo, López-Martin, Member IEEE, Carvajal, & Chavero, 2004; Torralba et al., 2009). This means that the gate made with POLY1 is not floating; on the contrary, it is connected to an external DC voltage level V_{ADJ}. This is shown in Figure 14. Eight external inputs (control gates, made with POLY2), labelled as $V_1, V_2, \cdots, V_8$, are capacitively coupled to the quasi-floating gate. The purpose of the external connection to the POLY1 layer is to adjust the offset of V_{OUT} in node 2 indicated in Figure 14, by adjusting V_{ADJ}. The input potential, Φ_{IN}, in the quasi-floating gate of the ν-NMOS transistor is given by Equation (3).

$$\Phi_{\mathrm{IN}} = v_{\mathrm{IN}} + V_{\mathrm{INoffset}} \tag{3}$$

where

$$v_{\mathrm{IN}} = \frac{C_k}{\delta_{\mathrm{f}} \cdot C_{\mathrm{T}}} \left(\sum_{k=1}^{8} V_k \right) \tag{4}$$

$$V_{\mathrm{INoffset}} = \gamma_{\mathrm{gd}} V_{\mathrm{DD}} + \gamma_{\mathrm{gs}} (a_{\mathrm{m}} \cdot V_{\mathrm{ADJ}} - V_{\mathrm{TH}}) \tag{5}$$

$\gamma_{\mathrm{gd}} = \frac{C_{\mathrm{gd}}}{\delta_{\mathrm{f}} \cdot C_{\mathrm{T}}}$ and $\gamma_{\mathrm{gs}} = \frac{C_{\mathrm{gs}}}{\delta_{\mathrm{f}} \cdot C_{\mathrm{T}}}$ are the coupling coefficients for the parasitic capacitances *gate-drain* and *gate-source*, respectively. The input signal v_{IN} is the weighted average due to the input from the neighbouring pixels. So the arithmetic average $\frac{1}{8} \sum_{k=1}^{8} V_k$ is mapped to $\frac{C}{\delta_{\mathrm{f}} \cdot C_{\mathrm{T}}} \left(\sum_{k=1}^{8} V_k \right)$ by the ν-NMOS neuron. Here δ_{f} is the feedback coefficient between the input and the output through the parasitic capacitance C_{gs}. Assuming that each control gate has the same size, then C_{k} is the coupling capacitance between the control gates and POLY1 (quasi-floating gate) and C_{T} is the sum of all capacitances, including the parasitic.

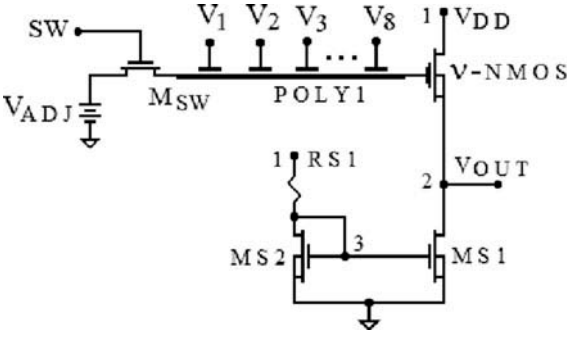

Figure 14. Schematic architecture for ν-NMOS neuron.

4.1.1. *v-NMOS neuron: analysis of output variables*

V_{OUT} is the neuron's response (node 2 in Figure 14) and is modelled by:

$$V_{OUT} = m_p \cdot \Phi_{IN} + V_{OF} \tag{6}$$

V_{OF} is an offset voltage level at the output of the v-NMOS neuron and m_p is simply a proportionality constant, considering that the neuron is an electronic circuit configured as a non-ideal source follower.

4.2. *Basic operation of the photo-transducer for sustained response*

The characteristic that defines a sustained or a transient response has been implemented from a photo-transducer as is shown in Figure 15. In the case of the photo-transducer for sustained response, its schematic diagram is shown in Figure 15(a). The integration time (I-T) is controlled by VSHU applied to the gate of MSHUT and the reset time (R-T) is controlled applying VRE to the gate of MREST. The role of Mdum is to minimise the digital noise introduced through VSHU and VRE. V_{outph} is the output of the photo-transducer which is expressed as:

$$V_{outph} = V_{offsetph} + \Delta V_{ph} \tag{7}$$

where

$$\Delta V_{ph} = \frac{1}{C_{ph}} \cdot i_{ph} \cdot \Delta t \tag{8}$$

ΔV_{ph} falls between the limits:

$$V_{rest} < \Delta V_{ph} < V_{DD} \tag{9}$$

and it can be assumed that inside this limit, i_{ph} is constant in time, for a given illumination value. One of the most important features in the architecture of the photo-transducer is that the stored potential at node N2 is sustained because it is floating when MSHUT is

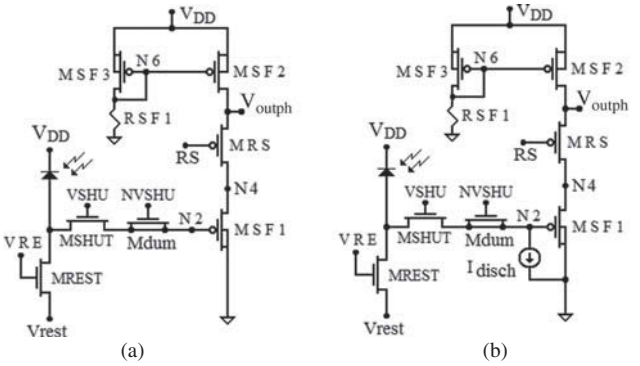

Figure 15. Photo-transducer: (a) With sustained response; (b) With transient response.

opened during the reading phase. The reading phase is set after the integration cycle, then it will be called sustained response.

4.2.1. *Basic operation of photo-transducer for transient response*

Since node N2 in Figure 15(a) sustains the potential stored while MSHUT is open (while reading phase), a discharge can be produced in this node in order to obtain a transient condition. In order to discharge node N2, a source current called I_{disch}, has been implemented as is shown in Figure 15(b). This current source was designed to discharge with a current in the order of pA.

$$\Delta V_{\text{N2}} = \frac{1}{C_{\text{ph}}} \cdot I_{\text{disch}} \cdot \exp(-K_{12} \cdot \Delta t) \tag{10}$$

$$V_{\text{outph}} = V_{\text{offsetph}} + \Delta V_{\text{ph}} \cdot \exp(-K_{12} \cdot t) \tag{11}$$

These equations are the same model as those given by cases 2 and 4 on Table 2.

4.3. *Comparator*

The schematic circuit of the comparator is shown in Figure 16(a). In regard to the comparator circuit, some features like the following can be mentioned: (1) for each value of V_{OUT} a transfer function like that shown in Figure 16(b) will result; (2) furthermore, if $V_{\text{outph}} > V_{\text{OUT}}$, the value of V_{out-c} (see Figure 16(a)) would be a high analog value; (3) if both, V_{outph} and V_{OUT} are small values, which represent a low illumination condition, then $V_{\text{out-c}}$ will have a low value; (4) finally, if both V_{outph} and V_{OUT} have high values, which represent a high and uniform illumination condition, then $V_{\text{out-c}}$ will have an intermediate value, not too high and not too low. These are features required for a dynamical comparator. The last three features are not shown in Figure 16 (b). As it can be seen in Figure 16(a), the comparator is designed with two mutually controlled current mirrors, one of them operating as a current sink and the second as a current source. The properties (1), (2), (3) and (4) previously specified are satisfied by the architecture of the comparator given in Figure 16(a). Here V_{outph} comes from the photo-transducer, and V_{OUT} from the neuron *v*-NMOS transistor. $V_{\text{out-c}}$ is the output from the

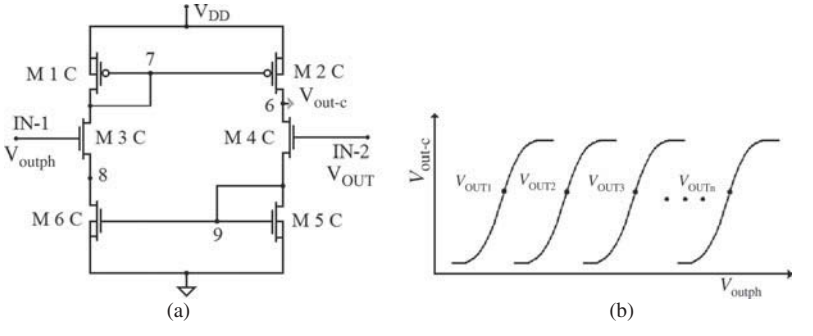

Figure 16. Comparator: (a) schematic; (b) ideal response.

comparator. Next, the second expression in Table 3 can be rewritten with new subscripts related now to the notation used in the schematic circuits; this is:

$$V_{\text{out}-c} = V_{\text{outph}} - V_{\text{OUT}} \tag{12}$$

with $V_{\text{out}-c} \equiv \Delta V_0$, $V_{\text{outph}} \equiv V_{5\text{th}}$, $V_{\text{OUT}} \equiv V_{\Omega}$. To avoid troubles with those values of $V_{\text{out}-c}$ less than 0.0 V ($V_{\text{out}-c} < 0$) in the model (12), we would consider to modify such model in the following way.

$$V_{\text{out}-c} = \left| V_{\text{outph}} - V_{\text{OUT}} \right| \tag{13}$$

From this last consideration, if both V_{outph} and V_{OUT} have small values, then $V_{\text{out}-c}$ has a small value. That corresponds to a low illumination condition. Moreover, if $V_{\text{OUT}} > V_{\text{outph}}$, then $V_{\text{out}-c} \rightarrow V_{\text{small}}$ which means that the area surrounding the centre receives highest illumination than the centre, and then, the neuron tends to have a smallest response. Then in turn, the neuron's response can be smaller than the neighbours' response if it is placed in the centre of a RF. That is not represented on the ideal characteristic from Figure 16(b).

4.4. *Oscillator*

Important features required for the oscillator are as follows. It can operate with frequencies below 10 kHz – it should be remembered that biological neurons work at very low frequencies (10–1 kHz). The second important feature is that the width of pulses can be adjusted to 100 μs. In this work, an oscillator which is voltage-controlled has been proposed, and its general architecture is shown in Figure 17. It is a kind of ring oscillator and is able to generate pulses at low frequencies. Each of the so-called *differential pair* is not an exactly symmetrical pair, since the difference between the aspect ratio of the input transistors (M2 and M3) is designed to produce an unbalanced condition resulting in oscillations. Frequency is controlled by the voltage INOSC which is the output from the comparator.

Oscillation is produced due to the difference in aspect ratios of M2 and M3. By adjusting the aspect ratio of M4 and M5, the width of the pulse can be controlled. For the case of sustained response, the frequency is given by:

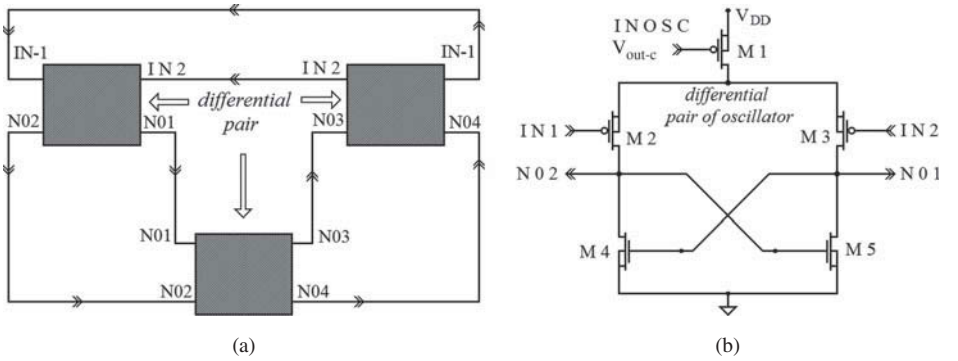

Figure 17. Oscillator: (a) block diagram; (b) schematic of each differential pair.

$$f_{on} = K^{+}_{ons} \cdot \Delta V_0 \tag{14}$$

This is the model for the response of the oscillator when it is excited with a signal that is started from a circuit like that shown in Figure 15(a). On the other hand, if the oscillator is excited with a signal that is started from a circuit like that shown in Figure 15(b), the response will be transient and this is modelled by Equation (15).

$$f_{ont} = f_{on} \cdot \exp(-K_{12} \cdot t) \tag{15}$$

Here $\Delta V_0 \equiv V_{out-c}$ is evaluated by the comparator, as stated earlier.

5. Simulations of electronic design

The simulations for each module mentioned in the previous sections – *v*-NMOS neuron, photo-transducer, comparator and oscillator – are presented.

5.1. *Results for the v-NMOS neuron*

Figure 18 shows the transfer function of a neuron v-NMOS. Figure 19 shows the floating-gate voltage of a v-NMOS as a function of V_1 taking V_2 as a parameter and keeping the other six inputs to ground. It can be seen from Figure 18 that if $V_{ADJ} = 1.6V$, the output from the v-NMOS transistor is almost the intrinsic threshold voltage (VT) value of 0.5 V. That means that when the weighted inputs $V_3, \cdots, V_8$ are above V_{TH} the neuron is fired. So, we can adjust V_{ADJ} in order to obtain an output purely due to weighted inputs. For example, V_{ADJ} could take values from 1.0 V to 3.0 V, according to the simulation shown in Figure 18. On the other hand, capacitances C and C_T as well as the constant δ_f are experimental values and can be evaluated in a future work. However, from the simulated data in Figure 19, it was possible to estimate the number $C/(\delta_f.C_T)$ having values ranging from 0.07 to 0.1, which is very near to 1/8, a value given in the first model in Table 3. Simulations were carried out by using model Ponce (Ponce, 2005). In the classical language, the response of neuron to some stimulus is called activation function (f_A), which in this work is the same as the transfer function (f_T) such as is shown as the vertical axis in the Figure 18.

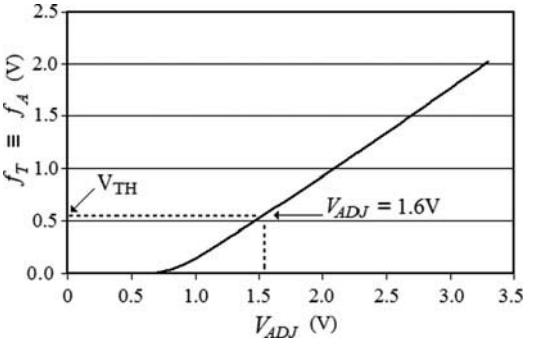

Figure 18. Transfer function (f_T) for the v-NMOS neuron, equivalent to the activation function (f_A).

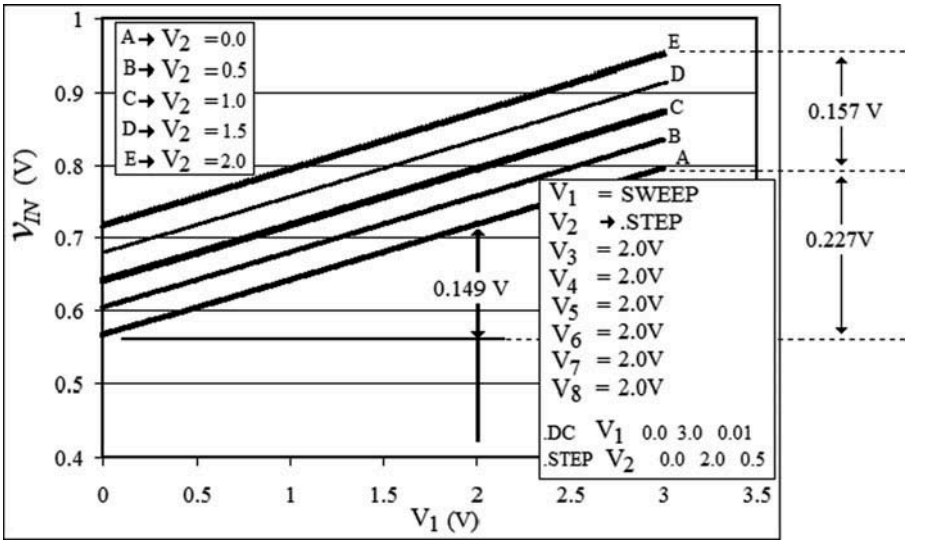

Figure 19. Floating gate voltage of ν-NMOS neuron, as a function of inputs $V_1, \cdots, V_8$.

5.2. *Results for the transducer*

From Figure 15(a) and (b), the photodiode's cathode has a highest voltage than its anode at the beginning of the I-T. Hence, due to the leakage current, node N2 tends to reach the voltage at node V_{DD}, namely, the voltage at node N2 grows from the level of V_{rest} to the level of V_{DD} during the I-T. Since the transducer is a source follower, its output is expected to be near the value present in node N2. Figures 20 and 21 show this behaviour. During the R-T, node N2 is set to V_{rest}, then the I-T starts. After this period, the hold time (H-T) is started, where reading or signal processing is carried out.

Comparing Figures 20 and 21, it is possible to see the difference of the signal on the windows of time H-T. This is the time where the response of the neuron is produced. Therefore, if the voltage is constant during that lapse of time, the frequency of the output

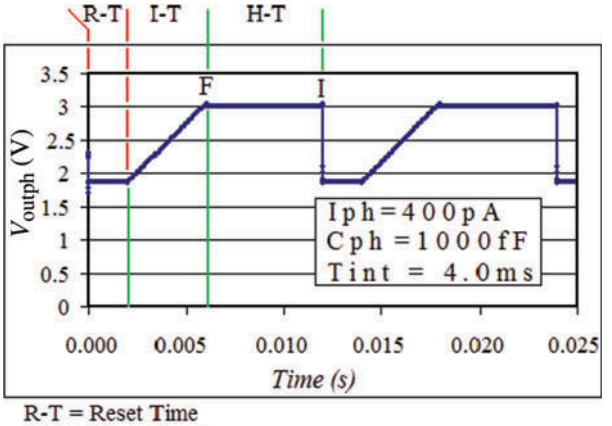

Figure 20. Response of the photo-transducer used on a receptive field with a sustained response.

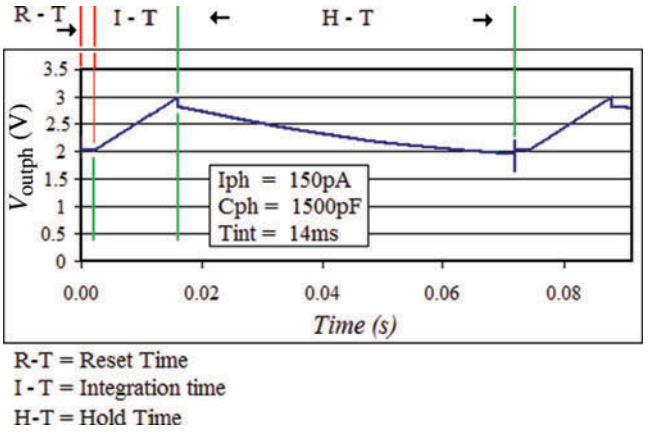

Figure 21. Response of the photo-transducer used on a receptive field with a transient response.

signal in the oscillator is constant. However, if the voltage has a discharge during the H-T, the frequency of the signal from the oscillator will be transient.

5.3. *Results for the comparator*

The inputs to the comparator are V_{OUT} and V_{outph}. V_{OUT} is the output from the *v*-NMOS neuron and V_{outph} is the output from the photo-transducer. Simulations of the comparator are shown in Figure 22. Here V_{OUT} is a parameter, with labels 0, 1, 2, 3, 4, 5, 6, 7 and 8, and V_{out-c} is the output from the comparator (Figure 16(a)). The horizontal axis is the signal coming from the photo-transducer.

There, when $V_{outph} > V_{OUT}$, the response is high, as is the case for the curve labelled as 6. If $V_{OUT} > V_{outph}$, the response always is low and the better example is the graphic with label 0. When both V_{outph} and V_{OUT} are low values (which belong to low illumination), the response is low. It is a dynamic evaluation of Equation (13). The most important feature is that it can be carried out by an analog methodology in hardware.

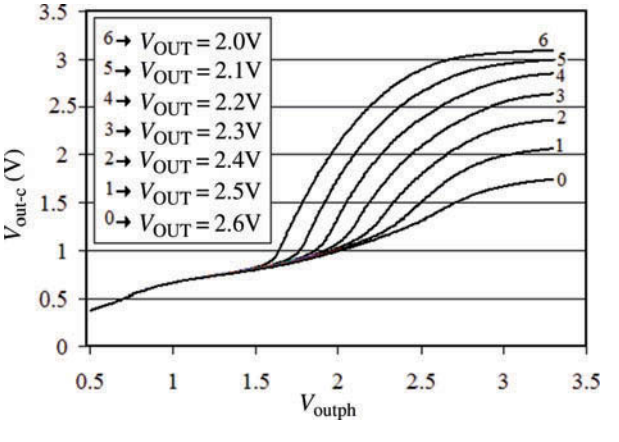

Figure 22. Parametric transfer function for the comparator.

5.4. *Oscillator's response*

As it was mentioned earlier, a RF has been implemented by means of a 3×3 pixel array. Each pixel has the four modules that were explained before. Here simulations for one of those RF are presented. At the same time, the response of the oscillator is presented. Results were excellent as is shown in Figure 23. These pulses are the response from the oscillator when surrounding photodiodes deliver 20 pA while the central region delivers 40 pA, with an I-T of 14 ms. The previous data belong to a centre with higher illumination. L3 is the output from the oscillator, L1 is the output from the photo-transducer and L2 is the output from the comparator. It should be remembered that the photocurrent is translated to voltage by the photo-transducer. The flat zone of Figure 23 is the reading time of 40 ms. The plot shown in Figure 23 corresponds to the pulses delivered by the oscillator from the simulation of the circuit whose description was given earlier. However, the response shown corresponds to the case when such oscillator is embedded inside a complete pixel and a RF, and furthermore, belongs to a kind of sustained response.

6. Measurements

Measurements were done to the fabricated chip (see Figure 24) whose design was previously described. The surface's circuit was covered with a layer of metal-3 in order to avoid a little of noise from substrate that can be introduced by external illumination. Each black point in the microphotograph is a window right above a photodiode on each pixel. The array of nine black point shows that there are nine pixels that form a RF. It should be remembered that each pixel is configured by the following blocks: photo-transducer, *v*-NMOS transistor, comparator and oscillator.

The photo-transducer was fabricated and characterised on other chip previously reported (Castillo-Cabrera, García-Lamont, Reyes Barranca, Moreno-Cadenas, & Escobosa-Echavarría, 2011). That was based on a *P* +/N-Well/P-substrate structure, made through an available commercial CMOS foundry (ON semiconductor). So, based on the knowledge obtained from this first characterisation, a second chip was designed and fabricated in order to characterise and evaluate the ν-NMOS neuron and the other three blocks whose designs have been explained previously. Figure 24 shows a

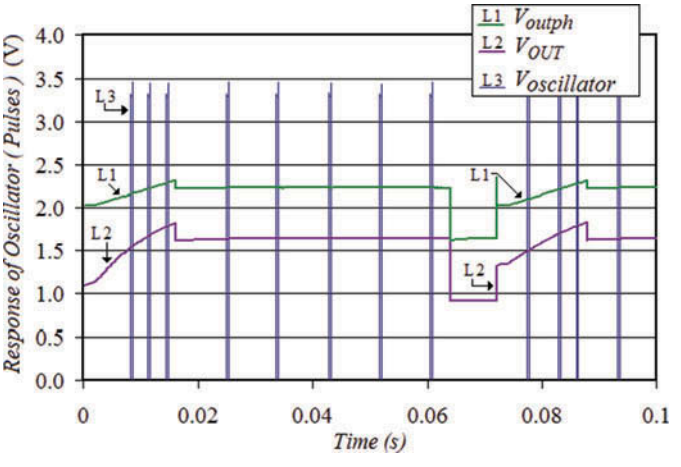

Figure 23. Pulses delivered by the oscillator.

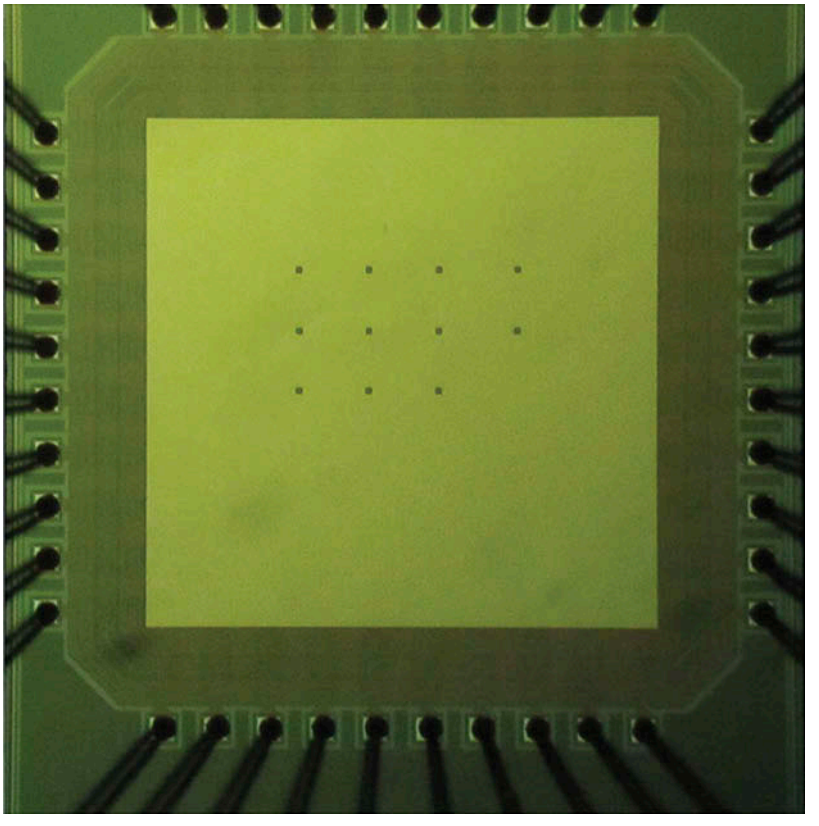

Figure 24. Chip's microphotograph from MOSIS run V03M-CJ.

microphotograph of the second chip and contains a 3×3 pixel array that emulates a RF. In addition, this second design contains coupler circuits that interconnect several functional blocks. Next, some measurements made to the chip are shown in Figure 24.

6.1. *Measurements from the photo-transducer*

Since some new elements were integrated inside the cell of the photo-transducer in this second design, measurements are shown in Figure 25. The I-Ts used are: (a) 1.0 ms, (b) 3.0 ms and (c) 6.0 ms. Also, three illumination powers were used: 0.0 μW/cm^2, 243 μW/cm^2 and 400 μW/cm^2. R-T was kept to 0.40 ms in all measurements.

Referring to Figure 25, H-T which is the same as the P-T is the time window when the analog processing is carried out. I-T is the time window where photocurrent is translated to voltage and is equivalent to the neuron's latency which is the 'neuron's recovery time'. H-T is the time window when the neuron FGMOS (*v*-NMOS) delivers its response.

6.2. *Measurements from a single v-NMOS neuron*

Here, the *v*-NMOS neuron is used as a quasi-FGMOS. In order to understand the measurement done, Figure 26 is repeated for convenience. Control inputs are V_1, V_2, …, V_8 and represent the signals coming from the neighbour pixels feeding the quasi-

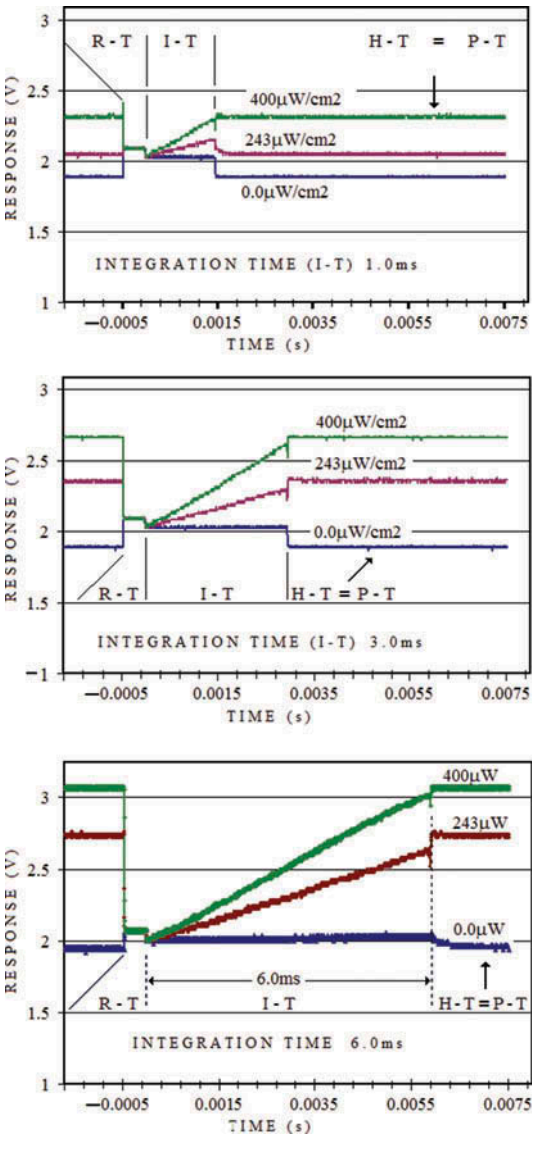

Figure 25. Measurements made to the photo-transducer at different integration times: (a) 1.0 ms; (b) 3.0 ms and (c) 6.0 ms.

FGMOS. The MSW transistor plays the role of a switch with which the VT of the *v*-NMOS neuron can be adjusted. A proper VT is adjusted applying an analog level V_{ADJ} to the layer of POLY1. A measurement from a single *v*-NMOS neuron is shown in Figure 27. The measurement was performed keeping inputs V_1, V_2,…, V_8 connected to the ground. An input pulse is applied to the layer POLY1 with the selected value for V_{ADJ} during 4.0 ms, after which it is turned off. Next, a logic '1' is applied to pin SW during 4.0 ms and then a logic '0' is applied after this time. The V_{ADJ} analog value applied to the layer of POLY1 was 1.0 V. A discharge is then observed during almost 80 seconds after the excitation. The output was measured at V_{OUT}. It is assumed that such discharge is due

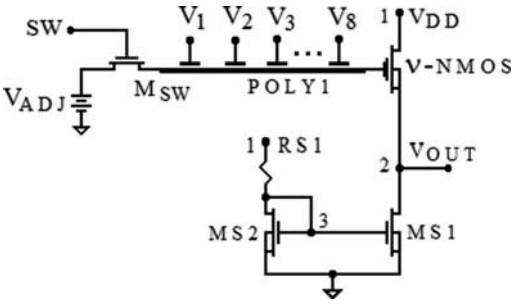

Figure 26. Configuration of the quasi-FGMOS v-NMOS neuron.

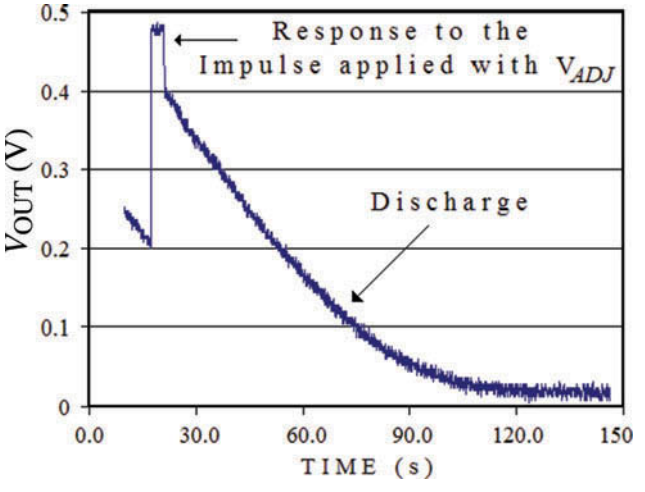

Figure 27. Response of the ν-NMOS neuron when a short pulse is applied to V_{ADJ}.

to leakage current through the switch MSW. On the other hand, a larger H-T is necessary to match the response of the transistor to the biological neuron, and this was achieved with about 100 ms. During that time, V_{OUT} could be assumed constant. Also, it should be remembered that V_{OUT} will be compared with V_{outph}, the output of the photo-transducer in the local pixel considered so far.

6.3. *Parametric measurements and response of the v-NMOS neuron*

Next, a description is given of the parametric stimulus, the measurements made and the respective response of the *v*-NMOS neuron. Figure 28 shows the stimulus pattern used with the neuron. At the bottom of this figure, the reset signal is also shown which is generated by a digital signal on SW, over the gate of MSW, with an enabling level with value V_{ADJ}. The reset pulses can take values ranging from 1.5 V to 3.0 V. After each reset pulse, the control inputs V_1, V_2,…,V_8 are enabled sequentially. After the first reset pulse, at the end of t_1, only V_1 is present and V_{OUT} is measured at this moment. After the second pulse, at the end of t_2, only inputs V_1 and V_2 are enabled, and then a measurement is made, and so on, this continues after completing the eight inputs pulses, such that at the end of t_8, all the eight inputs are enabled and a record of the response is made. Such

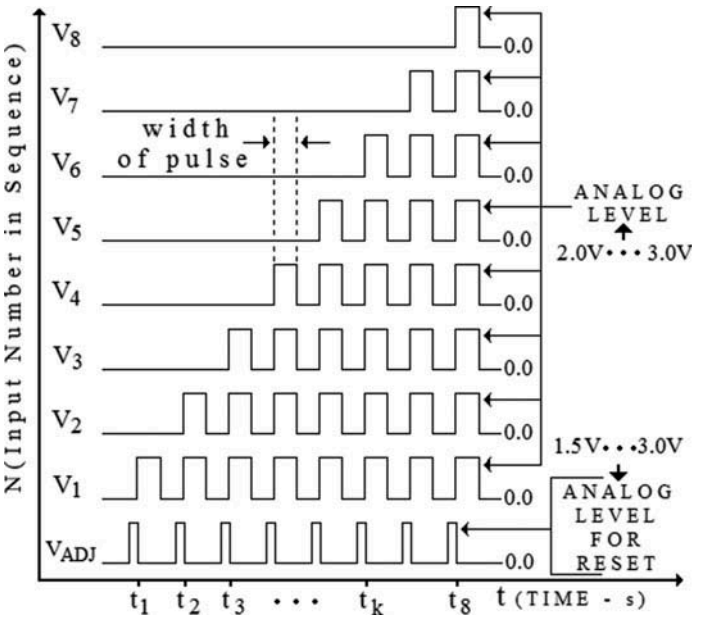

Figure 28. Pattern used for the stimulus in the control inputs of the ν-NMOS neuron.

control inputs can have analog levels ranging from 2.0 V to 30 V. This is an optimised interval, and it is excellent because it is matched with the output of each photo-transducer as is shown in Figure 25. Matching is desired since a good coupling must be done. The minimal high level width of the pulse for each control input must be equal to the I-T. This is the required time for 'recovery of the neuron', which is an equivalent concept for the biological counterpart. The latter description refers to the recommended width of each pulse for the analog level of control inputs V_1, V_2, …, V_8 in Figure 28.

Two typical measurements are shown in Figures 29 and 30. For the case shown in Figure 29, V_{ADJ} = 3.0 V, whereas for the case presented in Figure 30, V_{ADJ} = 2.0 V.

Due to V_{ADJ}, an offset level (V_{OFF}) is added to the output V_{OUT}. This offset was modelled by the following equations.

$$V_{OFF} = \alpha_{off} V_{ADJ} \tag{16}$$

and

$$V_{OUT} = \Phi_{OUT} + V_{OFF} \tag{17}$$

For this design, it was found that $\alpha_{off} \cong 0.51$. Here Φ_{OUT} is called 'the output signal' from the ν-NMOS neuron. Figure 31 shows values of V_{OUT} plotted as a function of the number of inputs (V_1, V_2,…,V_k). For example, line 'A' is the output when all the control inputs are biased at 1.0 volts each one, while V_{ADJ} is kept to 3.0V. This line 'A' is the same as shown in Figure 29. On the other hand, since the output of the photo-transducer will be compared with the output of the ν-NMOS neuron, the same voltage window is required in both the photo-transducer and the ν-NMOS neuron. From these measurements, a good matching is observed in their voltage windows. In Figure 25, a window

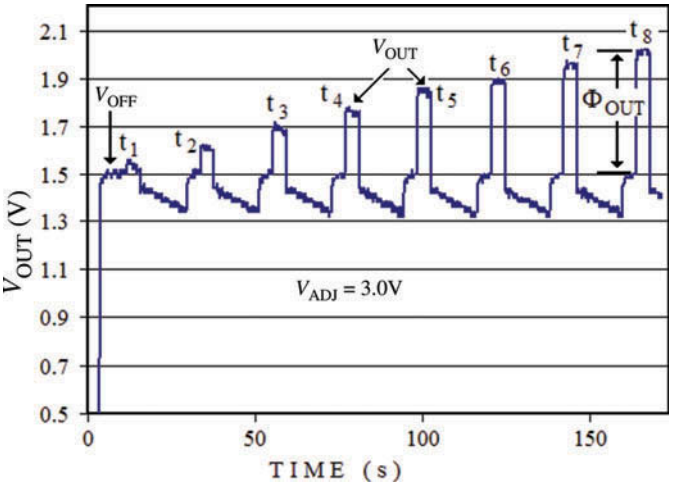

Figure 29. Measurements on node 2 for the ν-NMOS neuron of Figure 26, at V_{ADJ} = 3.0 V.

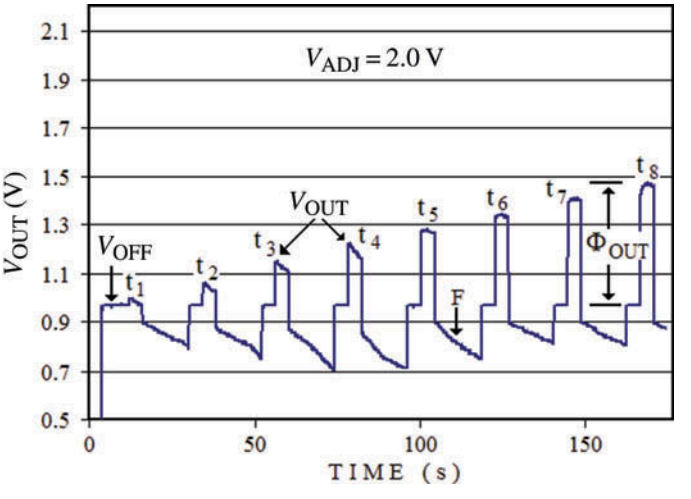

Figure 30. Measurements on node 2 for the ν-NMOS neuron of Figure 26, at V_{ADJ} = 2.0 V.

goes from 2.0 V to 3.0 V, while in Figure 31 this window goes from 1.7 V to 3.0 V. Measurements shown in Figure 31 can be compared with those measurements shown in Figure 25 to check these results. In addition, coupling can be checked in the same way between the output of the photo-transducer and the input of the *ν*-NMOS neuron to verify this agreement.

6.4. *Experimental data extraction*

From available technological parameters, the following parasitic and design capacitances were estimated: $C_k = 5.184\ fF$, $C_{gb} = 1.5\ fF$, $C_{gd} = 1.2\ fF$ and $C_{gs} = 16.598\ fF$, where C_k is the coupling capacitance for each POLY2 input; so, a correlation can be made

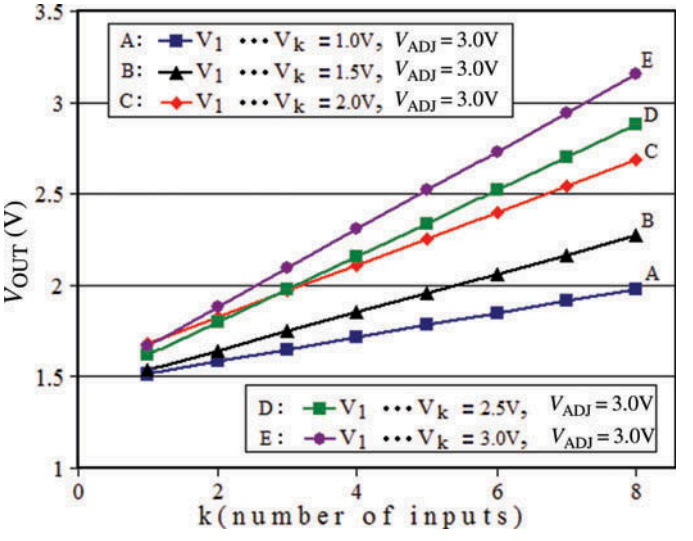

Figure 31. FGMOS output voltage measurements as a function of enabled control inputs.

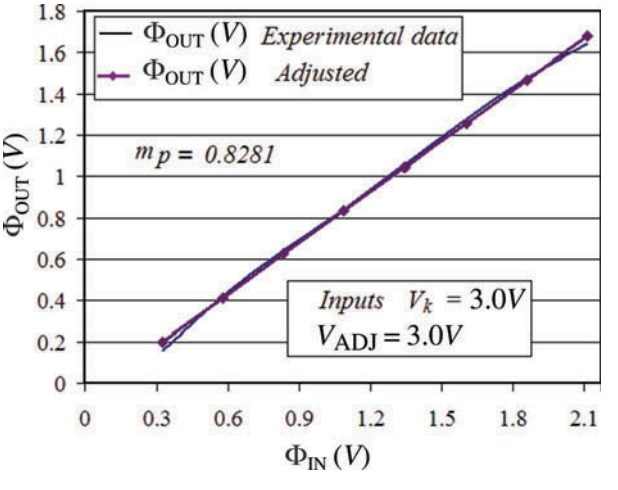

Figure 32. Correlation of data.

between Equation (6) and measurements shown in Figure 31. Figure 32 shows the output signal (Φ_{OUT}) versus the input signal (Φ_{IN}) where m_p from Equation (6) can be estimated. On the other hand, δ_f from Equation (4) can be calculated as follows: $\delta_f = 1 - m_p \frac{C_{gs}}{C_T} \cong 0.8$. Therefore, v_{IN} can be approximated to $v_{IN} \cong 0.1 \sum_{k=1}^{8} V_k$ where V_k is the value from each k_{th} input, coming from each neighbour.

7. Conclusions

In this work, it was shown how the FGMOS transistor or the so called *v*-NMOS neuron can be applied for analog processing tasks. The weighted sum of signals provided from the pixels is not exactly like a digital sum; however the nature is not necessary a digital sum. Within the input voltage range considered, the response of the *v*-NMOS neuron was linear, which simplifies the analysis for the performance of the circuit proposed. On the other hand, the discharge through transistor MSW due to leakage current across the junctions is long enough such that the P-T is not highly affected. Also, the voltage windows at the output of the FGMOS and the photo-transducer are in close agreement allowing proper operation of the comparator. The operation of the FGMOS transistor and the comparator are basic for the analog processing and the core of a RF block; however, the comparator and the oscillator need to be adjusted in order to obtain a pertinent operation of a RF block.

References

Castillo-Cabrera, G., García-Lamont, J., Reyes Barranca, M. A., Moreno-Cadenas, J. A., & Escobosa-Echavarría, A. (2011). Performance evaluation of an architecture for the characterisation of photo-devices: Design, fabrication and test on a CMOS technology. *International Journal of Electronics, 98*(3), 322–337. doi:10.1080/00207217.2010.538901

Chen, M., Weng, S., Deng, Q., Xu, Z., & He, S. (2009). Physiological properties of direction-selective ganglion cells in early postnatal and adult mouse retina. *The Journal of Physiology, 587*(4), 819–828. doi:10.1113/jphysiol.2008.161240

Cleland, B. G., Dubin, M. W., & Levik, W. R. (1971). Sustained and transient neurons in the cat's retina and lateral geniculate nucleus. *Journal of Physiology, 217*, 473–496.

Hartline, H. K. (1938). The response of single optic nerve fibers of the vertebrate eye to illumination of the retina. *American Journal of Physiology, 121*, 400–415.

Hubel, D. H., & Wiesel, T. N. (1959). Receptive fields of single neurones in the cat's striate cortex. *Journal Physiology, 148*, 574–591.

Hubel, D. H., & Wiesel, T. N. (1962). Organization of receptive fields in cat's visual cortex: Properties of "simple" and "complex" fields. Part I. *Journal of Physiology, 160*, 106–154.

Ichinose, T., & Lukasiewicz, P. D. (2005). Inner and outer retinal pathways both contribute to surround inhibition of salamander ganglion cells. *The Journal of Physiology, 565*(2), 517–535. doi:10.1113/jphysiol.2005.083436

Kilavik, B. E., Silveira, L. C. L., & Kremers, J. (2003). Centre and surround responses of marmoset lateral geniculate neurones at different temporal frequencies. *The Journal of Physiology, 546*(3), 903–919. doi:10.1113/jphysiol.2002.027748

Ponce, P. V. H. (2005) *Sensor Inteligente de Imágenes en Tecnología CMOS, con Aplicaciones en Robótica* (PhD thesis dissertation). CINVESTAV-IPN, Department of Electrical Engineering, Mexico City. Retrieved from http://sb3.csb.cinvestav.mx/uhtbin/cgisirsi/?ps=Yq9YJSbtG1/CENTRAL/6850005/123

Ramírez-Angulo, J., López-Martin, A. J., Member IEEE, Carvajal, R.G., & Chavero, F. M. (2004). Very low-voltage analog signal processing based on quasi-floating gate transistors. *IEEE Journal of Solid State Circuits, 39*(3), 434–442. doi:10.1109/JSSC.2003.822782

Shibata, T., & Ohmi, T. (1992). A functional MOS transistor featuring gate-level weighted sum and threshold operations. *IEEE Transactions on Electron Devices, 39*(6), 1444–1455. doi:10.1109/16.137325

Torralba, A., Luján-Martínez, C., Carvajal, R. G., Galán, J., Pennisi, M., Ramírez-Angulo, J., & López-Martín, A. (2009). Tunable linear MOS resistors using quasi-floating-gate techniques. *IEEE Transactions on Circuits and Systems II: Express Briefs, 56*(1), 41–45. doi:10.1109/TCSII.2008.2010163

Zhang, A.-J., & Wu, S. M. (2009). Receptive fields of retinal bipolar cells are mediated by heterogeneous synaptic circuitry. *The Journal of Neuroscience, 29*(3), 789–797. doi:10.1523/JNEUROSCI.4984-08.2009